Long-term in-use NO_x emissions from London buses with retrofitted NO_x aftertreatment

Napameth Phantawesak[a], Finn Coyle[b] and Marc E. J. Stettler[a]*

[a] Centre for Transport Studies, Department of Civil and Environmental Engineering, Imperial College London, SW7 2AZ, United Kingdom

[b] Transport for London, Palestra House, SE1 8NJ, United Kingdom

* Corresponding author: m.stettler@imperial.ac.uk

Abstract

Buses constitute a significant source of air pollutant emissions in cities. In this study, we present real-world NO_x emissions from 97 diesel-hybrid buses measured using on-board diagnostic (OBD) systems over 44 months and 6.35 million km in London. Each bus had previously been retrofitted with a selective catalytic reduction (SCR) aftertreatment system to reduce emissions of nitrogen oxides (NO_x). On average, parallel hybrid (PH) and series hybrid (SH) buses emitted 3.80 g/km (SD. 1.02) and 2.37 g/km (SD. 0.51) of NO_x, respectively. The SCR systems reduced engine-out emissions by 79.8% (SD. 5.0) and 87.2% (SD. 2.9) for the PHs and the SHs, respectively. Lower ambient temperatures (0 – 10°C) increased NO_x emissions of the PHs by 24.2% but decreased NO_x emissions of the SHs by 27.9% compared to more moderate temperatures (10 – 20°C). To improve emissions inventories, we provide new distance-based NO_x emissions factors for different ranges of ambient temperature. During the COVID-19 pandemic, the emissions benefits of reduced congestion were largely offset by more frequent route layovers leading to lower SCR temperatures and effectiveness. This study shows that continuous in-service measurements enable quantification of real-world vehicle emissions under a wide range of operations that complements conventional testing approaches.

Keywords: heavy-duty diesel vehicles, NO_x emissions, catalytic reactions, redox reactions, environmental pollution, temperature dependence, sensors.

Synopsis

Long-term monitoring of NO_x emissions from SCR retrofitted buses in London shows significant sensitivities to route average speed, traffic congestion and seasonal ambient temperature.

Graphical abstract

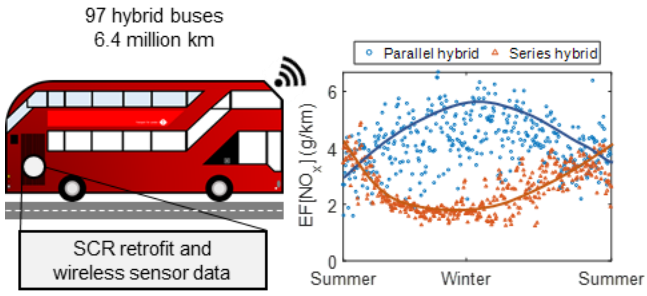

1 Introduction

1.1 Context

Transport is responsible for more than two thirds of all NO_x emissions in Europe (1). Road transport, including heavy-duty diesel vehicles (HDDVs), is a major source of nitric oxide (NO) and nitrogen dioxide (NO_2), collectively referred to as oxides of nitrogen (NO_x). In 2016, HDDVs contributed 30% and 19% of total NO_x emissions from the transport sector and total NO_x emissions in London, respectively (2). In 2020, diesel and diesel-hybrid buses represented more than 96% of the 9,102 London bus fleet (3).

Several studies have revealed that NO_x emissions from Euro IV and V HDDVs can be higher than approval limits in real-world driving conditions (4-9); up to 12.1 and 3.9 times the Euro IV and V standard, respectively. Retrofitting buses with selective catalytic reduction (SCR) aftertreatment systems has been shown to be an effective strategy for reducing NO_x emissions, and improving urban air quality, relatively rapidly and cheaply compared to the purchase of new vehicles (10-13). SCR systems comprise a catalyst in the exhaust, an injection system for adding a reductant in the form of a urea solution, commonly called diesel exhaust fluid (DEF), and sensors to control the injection rate. Injection of the reductant prior to the catalyst enables the reduction of NO_x to N_2 and water. Downstream of the SCR, an ammonia slip catalyst is typically required to oxidise potential emissions of excess ammonia (14). Following a 42% decrease in hourly NO_2 exceedances on Putney High Street kerbside as a result of retrofitting 93 buses in 2013 (13), an additional £85m has been invested in retrofitting 3,912 older buses with SCR to meet the Euro VI emissions standards since 2017 (3,15). These SCR retrofit technologies have been accredited through the

Clean Vehicle Retrofit Accreditation Scheme (CVRAS), which mandates a Euro VI equivalent NO_x limit of 0.5 g/km for approval. CVRAS accredited SCR retrofit technologies have been shown to reduce NO_x emissions of Euro V buses by more than 98%, from 14.5 – 26.3 g/km (pre-retrofit) to 0.1 – 0.3 g/km (post-retrofit), over the Millbrook London Transport Bus (MLTB) drive cycle on a chassis dynamometer (16).

The success of any retrofit strategy to reduce emissions is contingent on the effectiveness of emissions control devices across the fleet under typical operating conditions. Using remote sensing measurements, Liu et al. (17) found that 5% of buses contributed to 14% of the total NO_x emissions and Carslaw et al. (10) reported significant variation in emissions factors for earlier SCR retrofitted buses in London. Further, intentional tampering of SCR systems on Euro IV/V trucks was shown to increase NO_x emissions by 2.3 times (18). For studies that have used portable emissions measurement systems (PEMS), the number of vehicles that can be included in the study and the period over which they are monitored is typically limited (4,5,9,11,19). On-board diagnostics (OBD) that communicate real-time exhaust gas sensor outputs has made it feasible to monitor in-use vehicle emissions and SCR behaviour across a large fleet over a prolonged period (20,21). This is crucial for ensuring in-use compliance, elimination of aftertreatment tampering (18,21) and subsequently improving urban air quality.

Due to their perceived benefits, of greater fuel economy and lower emissions, hybrid buses now account for 41% of the 9,102 London bus fleet (3). In a parallel hybrid (PH), the wheels can be driven by (i) an internal combustion engine (ICE) alone, (ii) electric motor alone or (iii) both in parallel. In series hybrid (SH), however, the ICE output is first converted to electricity via a generator. The generated electricity then charges the battery or directly powers an electric motor to drive the wheels (22). While previous bus emissions studies have focused on parallel hybrid (PH) buses (4,5,23,24), there is a lack of evidence on the in-use NO_x emissions for series hybrid (SH) buses. Moreover, although the impact of ambient temperature on in-use NO_x emissions has been shown to be significant in light-duty diesel vehicles, with higher NO_x emissions typically observed at lower ambient temperatures (25,26), this remains largely understudied for HDDVs.

Accurate vehicle emissions inventories are critical to the development of air quality management strategies. At present, the most prevalent emission models categorise vehicles by type, size, fuel type and emissions standard and we note that emission factors for emerging technologies, such as

hybrid and SCR retrofitted buses, are currently not available in COPERT (27), HBEFA (28) nor MOVES (29).

1.2 Outline of paper

This paper presents an evaluation of real-world NO_x emissions from 97 Euro V SCR retrofitted buses, consisting of 23 PH and 74 SH buses. The objectives of this study are to: (i) quantify in-use NO_x emissions from SCR retrofitted buses operating on three routes over 44 months and 6.35 million vehicle-km; (ii) compare the emissions factors against a commonly used emissions model, COPERT, and previously reported emissions from MLTB test cycle; and (iii) evaluate the impact of external conditions on in-use emissions, including the effect of ambient temperature and the change in congestion levels due to the COVID-19 lockdown. Additional details omitted from the main text are included in the Supporting Information (SI).

2 Material and Methods

2.1 SCR bus fleet

The SCR bus fleet consisted of 97 buses from two manufacturers operating on three typical bus routes, which covered central London and suburban areas. Due to data sensitivity, the bus routes have not been disclosed. Table 1 presents a summary of vehicle specifications and OBD data collected in this study.

Table 1: Vehicle specifications of the SCR bus fleet and SCR parameters

	Parallel hybrid	**Series hybrid**
Manufacturer	Volvo	Wrightbus
Model	B5LH	New Routemaster
Emission standard	Euro V (original)	Euro V (original)

	Retrofitted to Euro VI	Retrofitted to Euro VI	
Emission control system	DPF + SCR retrofitted + ammonia slip catalyst	DPF + SCR retrofitted + ammonia slip catalyst	
Engine	Volvo D5F-215	Cummins ISB[e]	
Number of cylinders	4	4	
Engine displacement (L)	5	4.5	
Power (kW)	161	136	
Peak torque (Nm)	800	700	
Hybrid technology	I-SAM electric motor	Siemens ELFA II electric drive system	
Route and service time	A 24-hour service	B 5am - midnight	C 5am - midnight
Number of buses	23	46	28
OBD parameters	Vehicle speed [km/h], SCR inlet temperature [°C], mass air flow (MAF) [kg/h], urea injection rate [ml/h], engine-out and tailpipe NO_x [g/s and ppm]		

All buses were retrofitted with an emissions control system developed by Proventia under the trade name 'NO_xBUSTER® City DPF+SCR'. NO_x emissions and telematics data of the fleet, shown in Table 1 were recorded at 1 Hz frequency via the OBD systems. These parameters were retrieved from PROCARE™ Drive, a web-based tool for emissions monitoring. The efficacies of the SCR systems were monitored from October 2016, or as soon as the vehicles had been retrofitted, until the end of September 2019. All 97 buses were in operation (post-retrofit) for a minimum of 12 months and up to 36 months. The total distance covered by the fleet during this period was 4.96 million km.

Previous studies have reported strong correlations between on-board NO_x sensors and PEMS measurements. Tan et al. (20) reported a Pearson correlation coefficient of 0.98 for brake-specific NO_x emissions from HDDV trips on freeways. Cheng et al. (30) also found Pearson correlation coefficients of 0.76 – 0.87 and 0.95 – 0.99 for 1 Hz and 60-s moving average NO_x emission rates for trucks under various test conditions, respectively.

2.2 Ambient temperature data

Ambient temperature data from an observation site in Putney, London, UK, was used as a main reference for London's ambient temperature in this study. Where ambient temperature data from this observation site was not available, data from Heathrow Airport observation site was used to fill in the gaps. The data was retrieved from the Weather Observation Website (WOW MetOffice) (31) and combined with the OBD data to quantify the impact of ambient temperature on the SCR parameters listed in Table 1.

2.3 Data processing and analysis

2.3.1 Data quality

Typically, on-board NO_x sensors have an accuracy of ± 10 ppm from 0 – 100 ppm and ± 10% from 100 to 2,000 ppm (32). Therefore, we removed data where tailpipe NO_x emissions were greater than 1.1 times their corresponding engine-out NO_x to account for the accuracy and ammonia sensitivity of the NO_x sensors. Erroneous and missing OBD entries were also removed.

To ensure proper functioning of the SCR systems, days containing more than 3,600 consecutive seconds of 0 ml/h urea injection rate were interpreted as system malfunctions, for example due to sensor malfunction or insufficient urea, and removed from the main analysis. Due to the exclusion of this data, real-world NO_x emissions are likely to be higher than the emissions reported in this study and we recommend that future studies investigate the emissions when the on-board NO_x sensors are malfunctioning using PEMS. Further details on the process of data cleaning are presented in the SI §S1.2.

2.3.2 Distance-based NO_x emissions and COPERT estimates

OBD data in 1 Hz were divided into hourly segments by time (i.e. HH:00:00 – HH:59:59), and the hourly average speed, NO_x emissions factor, SCR temperature and ambient temperature were calculated for every vehicle. This generated 61,000 and 260,000 hourly data points for the PH and the SH buses, respectively. The distance-based NO_x emissions factor (in g/km) in each hour was calculated by dividing the total emissions in each hour by the distance travelled,

$$\mathrm{EF(NO_x)}\left[\frac{\mathrm{g}}{\mathrm{km}}\right] = \frac{\sum_{t_1}^{t_2}\mathrm{ER(NO_{x,TP})}}{\sum_{t_1}^{t_2} d} = \sum_{t_1}^{t_2}\frac{\mathrm{ER(NO_{x,TP})}}{v}, \quad (1)$$

where $ER(NO_{x,TP})$ is the emissions rate of tailpipe NO_x in g/s, v is the instantaneous speed in km/s, t_1 is the start of the hour (HH:00:00), t_2 is the end of the hour (HH:59:59) and d is the distance travelled.

The hourly average ambient temperature was used to categorise the hourly average speed, SCR temperature and NO_x emissions factor into three different ambient temperature categories: 0 – 10°C, 10 – 20°C and 20 – 30°C, to illustrate the impact of ambient temperature on NO_x emissions factor and SCR temperature. The mean of the hourly data points, in each speed and ambient temperature category, was used to represent a speed dependent distance-based in-use NO_x emissions and SCR temperature profile.

The latest COPERT 5 model was used to predict a speed dependent distance-based NO_x emissions profile of Euro V SCR and Euro VI buses (27). The vehicle type, size, fuel and the two Euro standard categories chosen in COPERT were 'Buses', 'Urban Buses Standard 15 – 18 ton', 'Diesel', 'Euro V SCR' and 'Euro VI', respectively.

The SCR effectiveness is defined as,

$$\text{SCR effectiveness (\%)} = \frac{\sum \mathrm{ER(NO_{x,EO})} - \sum \mathrm{ER(NO_{x,TP})}}{\sum \mathrm{ER(NO_{x,EO})}} \times 100, \quad (2)$$

where $ER(NO_{x,EO})$ is the emissions rate of engine-out NO_x in g/s.

2.4 In-use NO_x emissions during COVID-19 pandemic

To assess the impact of COVID-19 restrictions on bus NO_x emissions, we extended our study to include data from February to September 2020. Buses remained an essential mode of transport for

critical workers throughout the pandemic and travel restrictions on the general population fluctuated in response to changing COVID-19 infection rates. We evaluate changes in bus speeds and layovers (i.e. waiting periods at bus stops), which reflect changes in traffic congestion, and on SCR performance and tailpipe emissions. In addition to the 4.96 million km covered between October 2016 – September 2019, this added a further 1.39 million km, bringing the total distance covered by this study to 6.35 million km.

The percentage of route layover per day is the percentage of total layover time in day *i* divided by the total operation time in day *i*,

$$\text{Route layover}_i\ (\%) = \frac{\sum t_{\text{layover},i}}{t_{\text{end},i} - t_{\text{start},i}} \times 100\ , \quad (3)$$

where $t_{\text{start},i}$ and $t_{\text{end},i}$ are the start and the end of operation for day *i*, respectively.

3 Results and discussion

3.1 Inter-vehicle comparison of the SCR systems

We used a binning method to assess the variability in urea injection and SCR effectiveness across the two hybrid types. For both PH and SH buses, the urea injection rate is controlled by engine-out NO_x and SCR temperature (threshold >170°C). The effectiveness of the SCR at reducing engine-out NO_x was predominantly controlled by the SCR temperature and mass air flow (corresponding to the residence time in the catalyst).

The SCR systems were found to operate consistently across buses in the fleet and the time-weighted mean coefficient of variation in urea injection rate was 11.1% and 7.35% for the PHs and the SHs, respectively. Similarly, the time-weighted mean coefficient of variation in SCR effectiveness was 9.01% and 5.58% for the PHs and the SHs, respectively. Thus, there is less variability in the operation and effectiveness of the SCR systems on the SHs. This is because the engine on the SH is operated in three discrete modes (charge-depleting, slow charging, and fast charging, as discussed in Section 3.2) as distinct from the transient operation of the engine on the PHs. Further details of these results are presented in the SI §S2.1.

3.2 Average in-use NO_x emissions of parallel hybrid and series hybrid buses

The average speed of the PHs and the SHs was 11.1 km/h (SD. 0.8) and 11.8 km/h (SD. 0.3), and their average engine-out NO_x were 18.8 g/km (SD. 1.2) and 18.6 g/km (SD. 1.3), respectively. Despite their comparable engine-out NO_x, the average SCR temperature for the SHs (279°C, SD. 10) was higher than the PHs (250°C, SD. 9). This contributed to higher SCR effectiveness and lower tailpipe NO_x emissions for SHs (87.2%, SD. 2.9; 2.37 g/km, SD. 0.51) compared to PHs (79.8%, SD. 5.0; 3.80 g/km SD. 1.02). For comparison, a large remote sensing campaign in five UK locations by Ghaffarpasand et al. (33) reported an average NO_x emissions of 9 ± 1 g/km for Euro V and 2.25 ± 0.25 g/km for Euro VI buses. Thus, our results confirm that the SCR retrofits are able to reduce NO_x emissions of the Euro V PH and SH buses to 1.7 and 1.1 times the real-world NO_x emissions of Euro VI buses, respectively.

In general, SCR effectiveness was higher on the SH and NO_x emissions were 38% lower compared to the PH. This is due to the difference in the operation of the two hybrid systems, which led to a higher SCR temperature in the SH compared to the PH. In the PH, the vehicle is propelled by both the internal combustion engine and an electric motor. In the SH, however, the combustion engine drives an electric generator which provides electricity to the battery and the electric motor which drives the wheels. This allows the combustion engine in the SH to operate at specific optimal modes to improve fuel efficiency (34). The SHs in this study operate in three distinct modes: charge-depleting or fully electric operation (MAF = 0 kg/h), slow charging (MAF range: 80 – 130 kg/h) and fast charging (MAF range: 200 – 270 kg/h).

SCR effectiveness and density maps of the PH and the SH are shown in Figure 1a – Figure 1d. Figure 1c shows that the PH spends significant (> 50%) time with MAF in the range of 75 – 125 kg/h, which corresponds to low engine load when idling and travelling at low speed. In this range of MAF, the PH achieves an SCR effectiveness of ≥ 90% when the SCR temperature exceeds 250°C (Figure 1a). In contrast, the spread of the MAF for the SH is significantly smaller than the PH due to its non-transient operation, as shown in Figure 1b and 1d, which resulted in higher SCR temperature in the SH (279°C, SD. 10) compared to the PH (250°C, SD. 9). Furthermore, Figure 1d clearly shows a bimodal distribution corresponding to slow charging and fast charging modes of the SH. Note that Figure 1d does not show a third mode at MAF = 0 kg/h because there is no SCR effectiveness (i.e. both engine-out and tailpipe NO_x are equal to zero) when the SH is in a charge-depleting mode. The proportion of time under charge-depleting, slow charging and fast

charging mode for the SH is discussed further in Section 3.3. For MAF in the range of 75 – 125 kg/h (slow charging), the SH shows an SCR effectiveness of ≥ 90% when the SCR temperature exceeds 210°C, which is 40°C lower than the SCR temperature required to achieve the same level of effectiveness on the PH. This clearly highlights the advantage of non-transient operations: without transient changes in engine-out NO_x, SCR temperature and MAF, urea injection is more consistent and SCR effectiveness is higher.

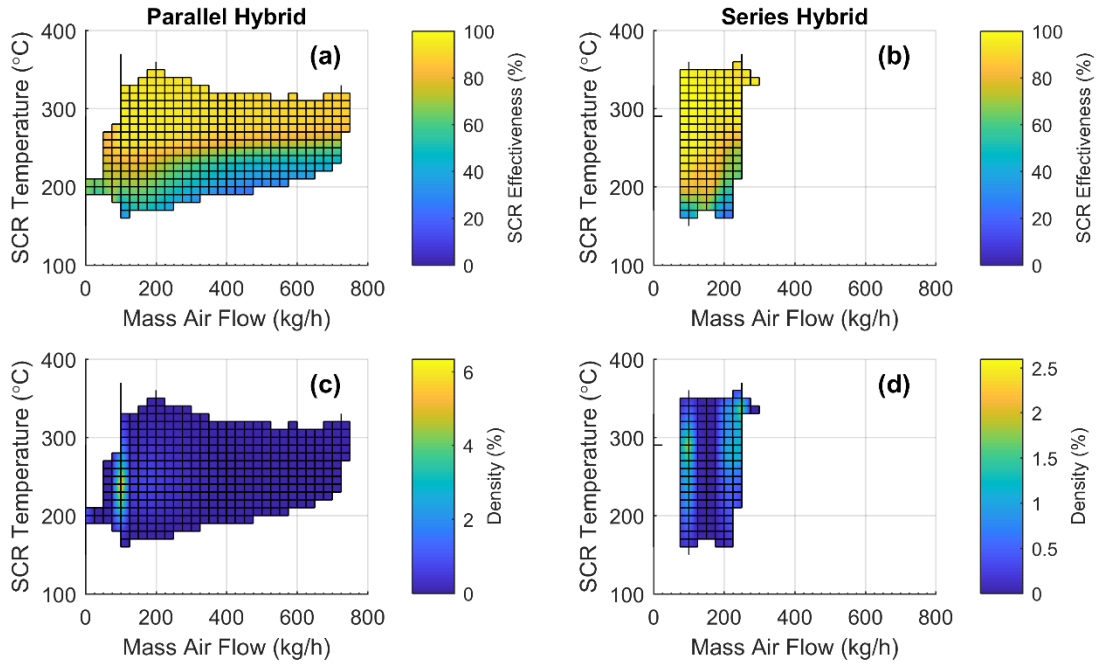

Figure 1: SCR effectiveness map of a) parallel hybrid (PH) and b) series hybrid (SH) buses, distribution of operation for c) PH and d) SH buses in bins of 25 kg/h mass air flow and 10°C SCR temperature.

The real-world tailpipe NO_x emissions for SHs (2.37 g/km, SD. 0.51) and PHs (3.80 g/km SD. 1.02) both exceed the 0.5 g/km Euro VI equivalent approval limit for the CVRAS accreditation (16). The CVRAS accreditation uses a chassis dynamometer test on the MLTB drive cycle (16), so to control for the effect of driving dynamics, we extracted real-world trips with driving characteristics including trip average speed, relative positive acceleration and 95th percentile of speed times positive acceleration ($(v.a_{pos})_{95}$) within ± 5% of the MLTB drive cycle. Note that these MLTB conditions do not represent the full distribution of driving dynamics experienced in real-

world conditions. When controlled for the driving characteristics of the MLTB cycle, the PHs and the SHs emitted 0.47 g NO_x/km (SD. 0.46) and 2.20 g NO_x/km (SD. 1.34), respectively. NO_x emissions of the PHs reduced by more than 85% compared to their average in-service emissions of 3.80 g/km (SD. 1.02), which suggests high sensitivity of the SCR effectiveness to the driving characteristics for the PHs. The SHs, however, were highly insensitive to the change in driving characteristics and the emissions did not change relative to their average in-service emissions of 2.37 g/km (SD. 0.51). Therefore, despite meeting the CVRAS Euro VI equivalent NO_x limit of 0.5 g/km during retrofit approval, our results show higher NO_x emissions when driven in real-world conditions compared to chassis dynamometer laboratory conditions. Moreover, our results also highlight significant variability in real-world NO_x emissions, even for buses of the same specifications, despite controlling for driving characteristics of the trips. Further details of the comparison are presented in the SI §S2.3.

One of the advantages of OBD measurements is the capability to measure in-service operation and the emissions of the fleet continuously over a prolonged period. Figure 2a – Figure 2c present the daily average speed, SCR effectiveness and NO_x emissions of the PHs and the SHs between October 2016 – September 2019, respectively.

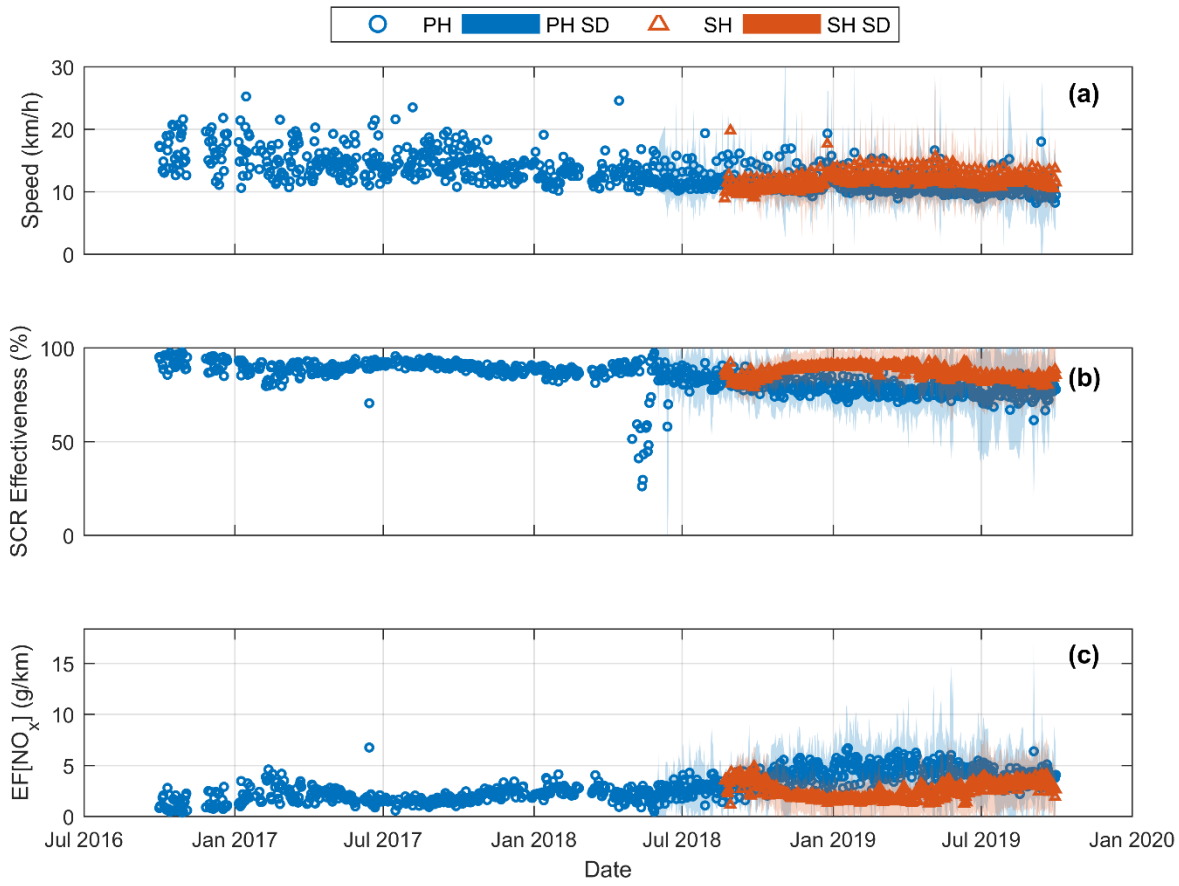

Figure 2: Daily average and 95% confidence interval (shaded areas, ±1.96×SD) of a) speed, b) SCR effectiveness and c) NO_x emissions of the PHs and the SHs between October 2016 – September 2019. The 95% CI starts when the number of vehicles is greater than 5.

The average speed of the PHs decreased from 16.8 km/h in October 2016 to 10.1 km/h in September 2019, as shown in Figure 2a. Consequently, the SCR effectiveness of the PHs decreased from 93.3% to 76.0% (Figure 2b), and NO_x emissions increased from 1.19 g/km to 3.95 g/km (Figure 2c) over the same period. Moreover, we found no evidence of SCR catalyst degradation over the period (shown in the SI §S2.3). These results highlight the negative impact of congestion on SCR effectiveness and NO_x emissions.

For the SHs, a temporary reduction in NO_x emissions around January 2019 (Figure 2c) could be attributed to a combination of an increase in average speed (Figure 2a) and lower NO_x emissions at lower ambient temperature for the SH. The impact of average speed and ambient temperature

on SCR effectiveness, and therefore NO_x emissions, are discussed further in section 3.4 and section 3.3, respectively.

3.3 Effects of ambient temperature

The effects of ambient temperature on NO_x emissions were found to be highly dependent on the type of hybrid system of the vehicle. Lower ambient temperature resulted in higher NO_x emissions in the PH but lower NO_x emissions in the SH. Ambient temperature had a direct impact on the production of engine-out NO_x and the SCR temperature, and, in turn, the SCR effectiveness and tailpipe NO_x emissions. Figure 3a – Figure 3f show the impact of ambient temperature on the mode

282 of operation, SCR temperature, engine-out NO_x, tailpipe NO_x emissions and SCR effectiveness of
283 the PH and the SH.

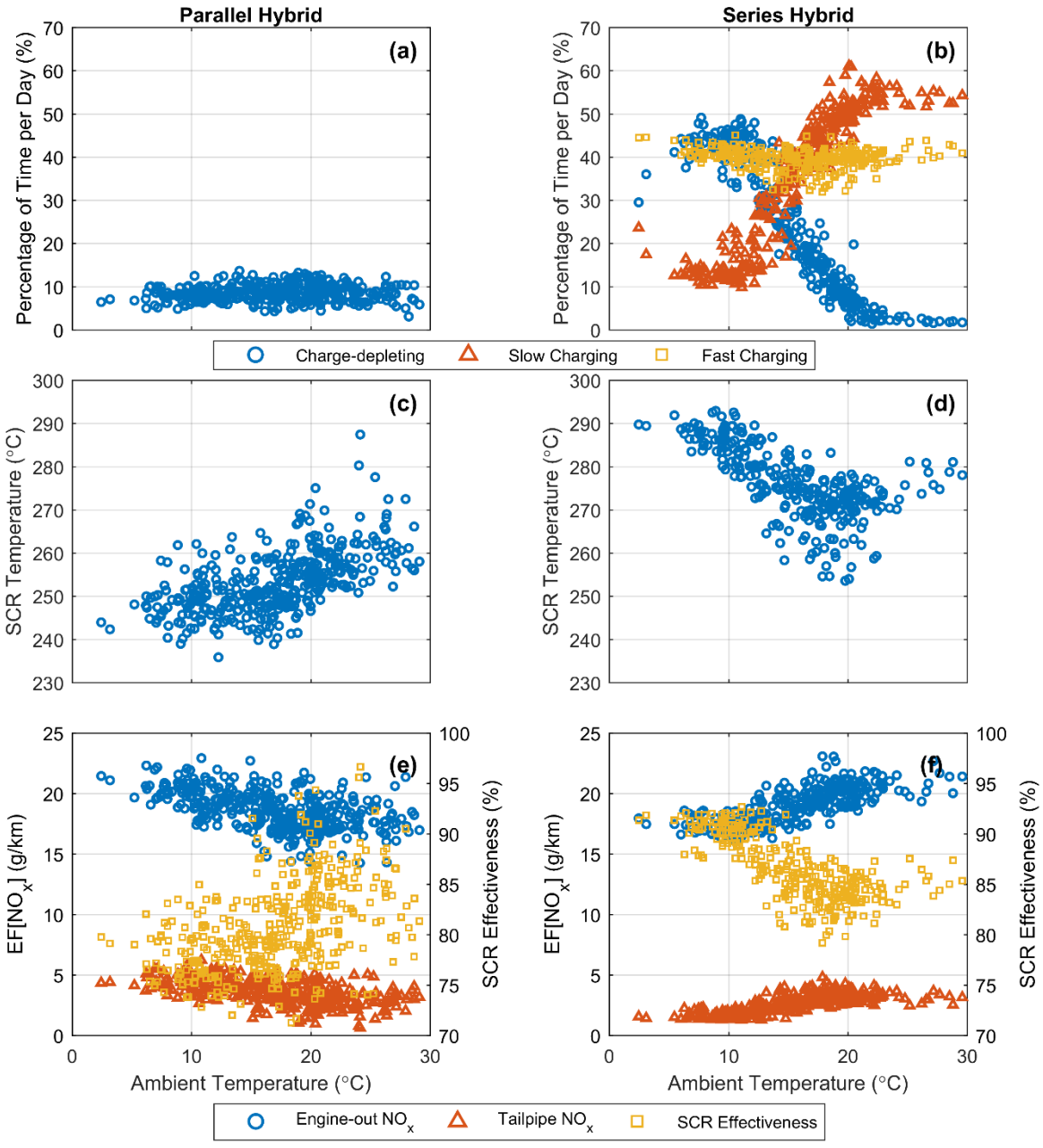

284

285 **Figure 3: a) Percentage of time per day under charge-depleting mode for PH, b) percentage**
286 **of time per day under charge-depleting, slow charging and fast charging mode for SH, daily**
287 **average SCR temperature for c) PH and d) SH, engine-out NO_x, tailpipe NO_x and SCR**
288 **effectiveness for e) PH and f) SH as a function of daily average ambient temperature.**

For the PH, higher engine-out NO_x (in g/km) was observed at lower ambient temperatures, which can be attributed to poor mixing of fuel and air, and lower combustion efficiency (35). We also observed an average reduction of 0.8°C in SCR temperature per 1°C reduction in ambient temperature. Together, higher engine-out NO_x and lower SCR temperature resulted in lower SCR effectiveness and elevated NO_x emissions in the PH at lower ambient temperatures.

In contrast, Figure 3 shows that the SH displayed lower daily average engine-out NO_x (in g/km) and higher SCR temperatures at lower ambient temperatures, resulting in higher SCR effectiveness and lower tailpipe NO_x emissions. This is due to the difference in the proportion of time spent in each operating mode (charge-depleting/slow charging/fast charging) at different ambient temperatures, as shown clearly in Figure 3b and further in the SI §S2.4. In colder temperatures (0 – 10°C), the SH spent the largest proportion of time per day in the fast charging mode (45%), more time in charge-depleting mode (40%) and less time under slow charging mode (15%) compared to warmer conditions. This is likely due to the adverse effect of low temperatures on the capacity and greater internal impedance of the battery (36). For higher ambient temperature, the charge-depleting mode is gradually substituted by the slow charging mode. This indicates greater consumption of electricity as ambient temperature increases, which could be attributed to the use of electrical accessories, such as air conditioning. Larger proportion of time under slow-charging mode resulted in higher engine-out NO_x (in g/km) in warmer conditions as the engine is on for a longer period. Moreover, the slow charging mode also has a greater cooling effect on the SCR compared to charge-depleting mode, which is reflected by a correlation between the percentage of time under charge-depleting mode (Figure 3b) and SCR temperature (Figure 3d), i.e. more charge-depleting and less slow charging resulted in higher SCR temperature and vice versa. Although lower ambient temperatures resulted in an overall reduction in NO_x emissions (in g/km) for the SH, we did not have the data to quantify if there was any impact on fuel consumption (5,24). There is limited existing literature that quantifies the effect of ambient temperature on SH bus NO_x emissions and while Kotz et al. (37) observed an increase in power-specific emissions with decreasing temperature, Keramydas et al. (38) observed a decrease in distance- and power-specific NO_x emissions with decreasing temperature. Future research should further explore the operation of the hybrid systems in response to ambient temperature for different vehicle specifications (e.g.

SH engine size and battery capacity), electricity power demand of the accessories and in-vehicle temperature setpoints.

We also divided the MLTB-like trips from Section 3.2 into different ambient temperature ranges to evaluate the impact of ambient temperature on NO_x emissions under the same driving conditions. The results show the same trend as observed for the full dataset in Figure 3. Details are presented in the SI §S2.3.

3.4 Distance-based NO_x emissions factors

Average-speed dependent distance-based NO_x emissions factors for the PH and the SH are presented in Figure 4a and 4b, respectively. The emissions factors are divided into three different ambient temperature categories to illustrate the impact of ambient temperature on the distance-based emissions factors, which are currently not accounted for in the emissions inventories.

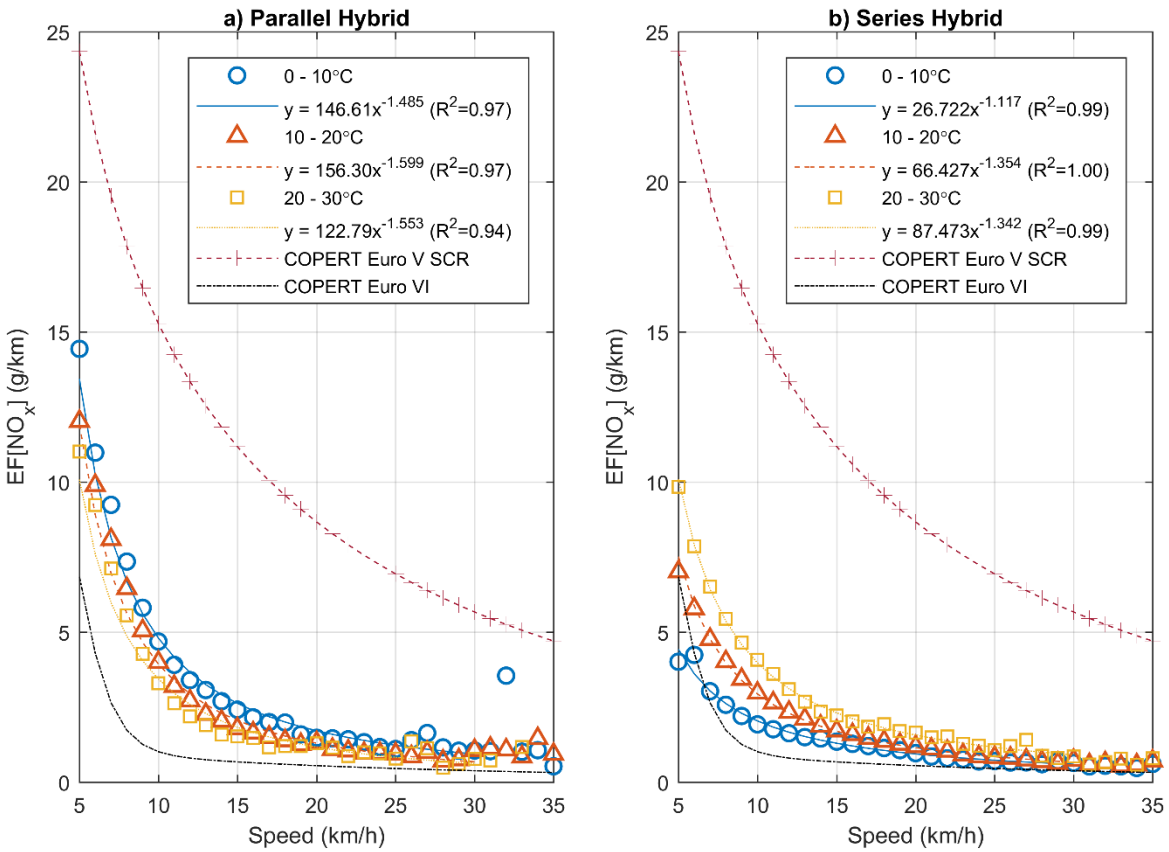

Figure 4: Distance-based in-use NO_x emissions factors of the a) PH and b) SH for three ambient temperature categories, as a function of hourly average speed. The mean ambient temperature encountered by the PHs and the SHs were 16.5°C (SD. 6.3) and 15.5°C (SD. 5.8), respectively. The power law fits were calculated based on speed between 5 – 30 km/h, as this represents 99.9% and 99.7% of the data for the PHs and the SHs, respectively. The number of data points, 5th and 95th percentile of the distance-based in-use NO_x emissions are presented in the SI §S2.5. The SCR temperature profiles are also presented in the SI §S2.5. COPERT 5 emissions factors provided for comparison.

Average speed was found to be a good proxy for in-use NO_x emissions in a one-hour period, resulting in R^2 between 0.94 – 1.00. This is predominantly due to the strong correlation between average speed and SCR temperature (shown in the SI §S2.5). The 90% confidence interval of the NO_x emissions factors are presented in the SI §S2.5 for quantification of emissions variability of the fleet. At a fleet average speed of 11.7 km/h, COPERT estimates 13.6 g NO_x/km and 0.82 g NO_x/km for Euro V SCR and Euro VI, respectively. At the same average speed, the power law fits for the PH and the SH at ambient temperature between 10 - 20°C provides an average in-use NO_x emissions of 3.04 g/km and 2.37 g/km, respectively. The discrepancy between in-use NO_x emissions and COPERT predictions highlights the usefulness of in-use monitoring data to keep emissions models up to date as new technologies emerge.

As ambient temperature decreased from 10 – 20°C to 0 – 10°C, NO_x emissions for the PH increased by 24.2%, from 3.04 g/km to 3.78 g/km. However, the same reduction in ambient temperature resulted in a 27.9% decrease in NO_x emissions for the SH, from 2.37 g/km to 1.71 g/km. Our result shows that the addition of ambient temperature categories, as illustrated in Figure 4a and 4b could further improve the estimate of distance-based emissions models for SCR hybrid buses in different climates.

When the two hybrid systems are compared in the same ambient temperature range, the distance-based in-use NO_x emissions of the SH (Figure 4b) are lower compared to the PH (Figure 4a) at ambient temperature between 0 - 10°C and 10 - 20°C. However, the SH becomes more polluting than the PH at ambient temperature between 20 - 30°C. Details of the comparison are presented in the SI §S2.5.

3.5 In-use NO_x emissions during the COVID-19 pandemic

In February 2020 (pre-lockdown), the average speed of the PHs and the SHs were 8.84 km/h and 11.9 km/h, respectively. Following the UK's lockdown on 23rd March 2020, the average speed of the routes between April – September 2020 increased by as much as 22.1% for the PHs and 26.1% for the SHs compared to pre-lockdown. To illustrate the effects of lockdown on SCR buses while accounting for the opposing effects of ambient temperature on NO_x emissions of the PH and the SH, Figure 5a – Figure 5f present both the monthly averages in 2020 and the year over year (YoY) percentage change in monthly average speed, SCR temperature, SCR effectiveness, NO_x emissions, ambient temperature and route layover in 2020 relative to 2019, respectively.

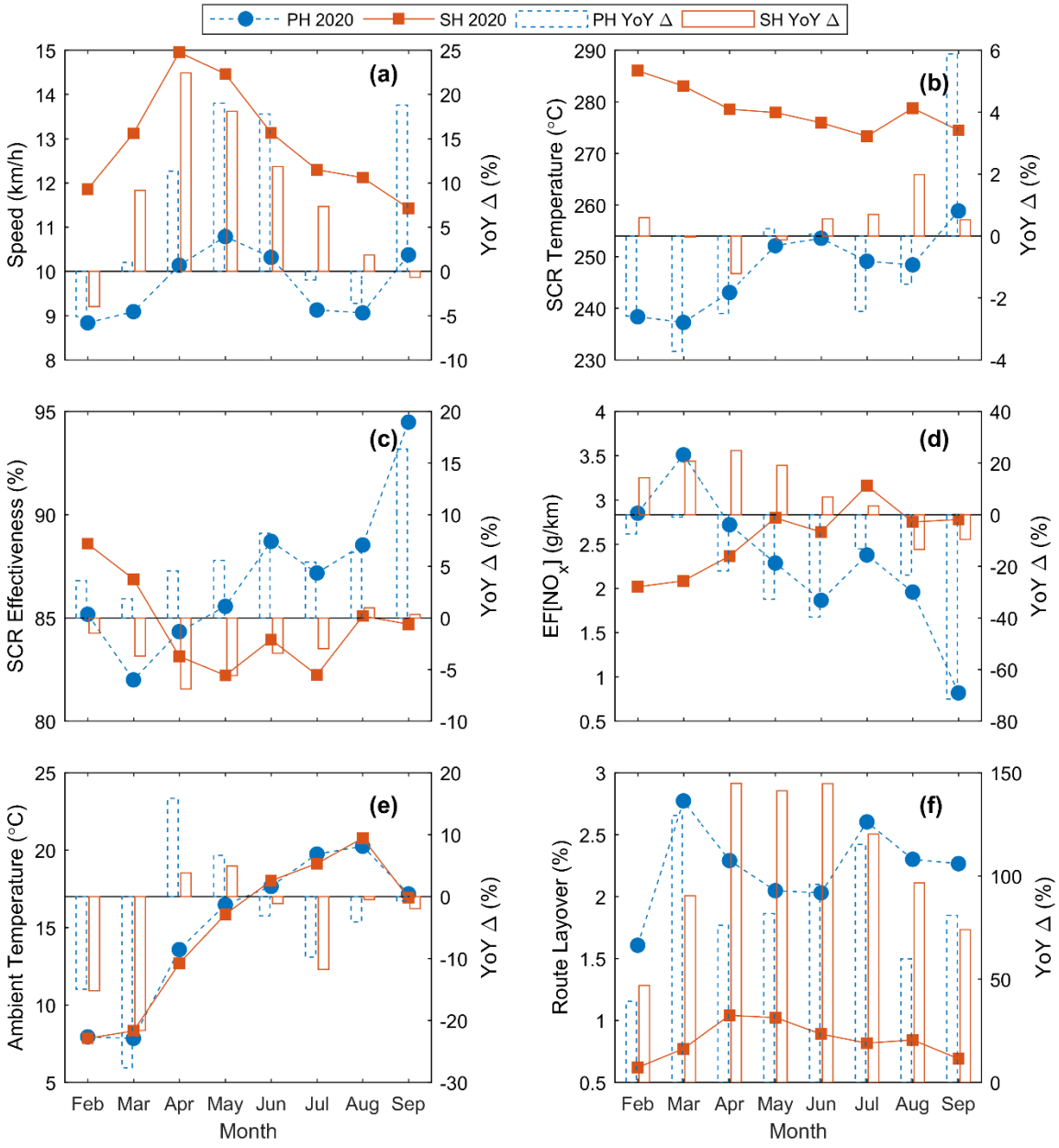

372

373 **Figure 5: Monthly averages in 2020 and year over year percentage change (YoY Δ) in**
374 **monthly average a) speed, b) SCR temperature, c) SCR effectiveness, d) NO_x emissions, e)**
375 **ambient temperature and f) route layover from 2019 to 2020.**

376

Despite significant changes in ridership (39), engine-out NO_x emissions were similar in 2020 compared to 2019 (see SI §S2.6). The expected reduction in tailpipe emissions due to reduced congestion was largely offset by a significant increase in route layovers (Figure 5f). Longer and more frequent waiting periods at bus stops exacerbated the cooling down of SCR temperature, which resulted in lower SCR effectiveness and elevated NO_x emissions at the beginning of each route. Once the buses are running, however, lower congestion allowed the PHs and the SHs to reach higher speed, thus, providing higher SCR temperature, higher SCR effectiveness and lower NO_x emissions in the latter portion of the route compared to pre-lockdown. Therefore, this creates a counterbalance between the elevated NO_x emissions at the start of each route due to route layover and the emissions reduction benefits from reduced congestions for the rest of the route.

When compared to the same period in 2019, the monthly average speed of the PH in April – September 2020 increased by 10.4% (SD. 8.7) YoY and NO_x emissions decreased by 33.7% (SD. 17.4) YoY. Similarly, the monthly average speed for the SHs also increased by 10.2% (SD. 8.3) compared to the same period in 2019. However, this was offset by a 120% (SD. 27) increase in route layover YoY. As a result, the SHs emitted 5.22% (SD. 13.85) more NO_x (in g/km) in April – September 2020 compared to the same period in 2019. Detailed month-to-month and YoY comparisons of Figure 5 are provided in the SI §S2.6.

Overall, the comparison of NO_x emissions during the COVID-19 pandemic against the same period in 2019 highlights the complexity in managing bus route characteristics to improve SCR effectiveness and reduce NO_x emissions. Our analysis shows that reducing congestion and route layover are only partly beneficial on their own. However, neither interventions are as effectiveness as using both interventions together to reduce NO_x emissions from SCR retrofitted buses.

In summary, our results suggest that reducing congestion (improving route average speed) and the change of bus timetabling to reduce route layovers should be done together to reduce NO_x emissions from the SCR bus fleet. Continuous in-service measurements of the telematics and NO_x emissions of the fleet via OBD can help detect and manage this.

The authors declare no competing financial interest.

Supporting Information

(1) Data cleaning procedure; (2) methodology and comparison of urea maps and SCR effectiveness maps; (3) average, SD and 90% confidence interval of SCR parameters (4) comparison of in-use NO_x emissions and MLTB drive cycle; (5) effects of ambient temperature; (6) detailed distance-based NO_x emissions factors and (7) further discussion on emissions during COVID-19.

Acknowledgements

We would like to thank Transport for London and Proventia for the provision of data. Napameth's PhD is funded by the Royal Thai Government.

References

(1) European Environment Agency. Emissions of air pollutants from transport. 2019; Available from: https://www.eea.europa.eu/data-and-maps/indicators/transport-emissions-of-air-pollutants-8/transport-emissions-of-air-pollutants-8.

(2) London Atmospheric Emissions Inventory (LAEI) 2016. 2020; Available from: https://data.london.gov.uk/dataset/london-atmospheric-emissions-inventory--laei--2016 [Accessed 4 February 2021].

(3) Transport for London. Bus fleet audit 31 March 2020. 2020; Available from: https://tfl.gov.uk/corporate/publications-and-reports/bus-fleet-data-and-audits [Accessed 30 July 2020].

(4) Guo, J.; Ge, Y.; Hao, L.; Tan, J.; Peng, Z.; Zhang, C. Comparison of real-world fuel economy and emissions from parallel hybrid and conventional diesel buses fitted with selective catalytic reduction systems. *Applied Energy.* 2015; 159 433-441. Available from: https://doi.org/10.1016/j.apenergy.2015.09.007.

(5) Zhang, S.; Wu, Y.; Hu, J.; Huang, R.; Zhou, Y.; Bao, X.; Fu, L.; Hao, J. Can Euro V heavy-duty diesel engines, diesel hybrid and alternative fuel technologies mitigate NO_x emissions? New evidence from on-road tests of buses in China. *Applied Energy.* 2014; 132 118-126. Available from: https://doi.org/10.1016/j.apenergy.2014.07.008.

(6) Anenberg, S. C.; Miller, J.; Minjares, R.; Du, L.; Henze, D. K.; Lacey, F.; Malley, C. S.; Emberson, L.; Franco, V.; Klimont, Z.; Heyes, C. Impacts and mitigation of excess diesel-related

NO_x emissions in 11 major vehicle markets. *Nature.* 2017; 545 (7655): 467. Available from: https://doi.org/10.1038/nature22086.

(7) Wu, Y.; Zhang, S. J.; Li, M. L.; Ge, Y. S.; Shu, J. W.; Zhou, Y.; Xu, Y. Y.; Hu, J. N.; Liu, H.; Fu, L. X.; He, K. B.; Hao, J. M. The challenge to NO_x emission control for heavy-duty diesel vehicles in China. *Atmospheric Chemistry and Physics.* 2012; 12 (19): 9365-9379. Available from: https://doi.org/10.5194/acp-12-9365-2012.

(8) Lowell, D.; Kamakaté, F. Urban off-cycle NO_x emissions from Euro IV/V trucks and buses. *The International Council on Clean Transportation.* 2012; Available from: https://theicct.org/publications/urban-cycle-nox-emissions-euro-ivv-trucks-and-buses.

(9) Fu, M.; Ge, Y.; Wang, X.; Tan, J.; Yu, L.; Liang, B. NO_x emissions from Euro IV busses with SCR systems associated with urban, suburban and freeway driving patterns. *Science of The Total Environment.* 2013; 452-453 222-226. Available from: https://doi.org/10.1016/j.scitotenv.2013.02.076.

(10) Carslaw, D. C.; Priestman, M.; Williams, M. L.; Stewart, G. B.; Beevers, S. D. Performance of optimised SCR retrofit buses under urban driving and controlled conditions. *Atmospheric Environment.* 2015; 105 70-77. Available from: https://doi.org/10.1016/j.atmosenv.2015.01.044.

(11) Smit, R.; Keramydas, C.; Ntziachristos, L.; Lo, T.; Ng, K.; Wong, H. A.; Wong, C. K. Evaluation of real-world gaseous emissions performance of selective catalytic reduction and diesel particulate filter bus retrofits. *Environmental Science & Technology.* 2019; 53 (8): 4440-4449. Available from: https://pubs.acs.org/doi/abs/10.1021/acs.est.8b07223.

(12) Chong, U.; Yim, S. H. L.; Barrett, S. R. H.; Boies, A. M. Air Quality and Climate Impacts of Alternative Bus Technologies in Greater London. *Environmental Science & Technology.* 2014; 48 (8): 4613-4622. Available from: https://doi.org/10.1021/es4055274.

(13) Barratt, B.; Carslaw, D. C. Impacts of the Bus Retrofit Programme on NO_2 Concentrations along Putney High Street. *King's College Environmental Research Group.* 2014. Available from: http://londonair.org.uk/london/reports/PHSSCRImpactsReport.pdf.

(14) Maunula, T.; Tuikka, M.; Wolff, T. The Reactions and Role of Ammonia Slip Catalysts in Modern Urea-SCR Systems. *Emission Control Science and Technology.* 2020; 6 (4): 390-401. Available from: https://doi.org/10.1007/s40825-020-00171-1.

(15) Transport for London. London's buses now meet ULEZ emissions standards across the entire city. 2021; Available from: https://tfl.gov.uk/info-for/media/press-releases/2021/january/london-s-buses-now-meet-ulez-emissions-standards-across-the-entire-city [Accessed 28 January 2021].

(16) Daniel Hayes. The clean vehicle retrofit technology guide. 2019; Available from: https://energysavingtrust.org.uk/service/clean-vehicle-retrofit-accreditation-scheme/ [Accessed 3 February 2021].

(17) Liu, Q.; Hallquist, Å. M.; Fallgren, H.; Jerksjö, M.; Jutterström, S.; Salberg, H.; Hallquist, M.; Breton, M. L.; Pei, X.; Pathak, R. K.; Liu, T.; Lee, B.; Chan, C. K. Roadside assessment of a modern city bus fleet: Gaseous and particle emissions. *Atmospheric Environment: X.* 2019; 3 100044. Available from: https://doi.org/10.1016/j.aeaoa.2019.100044.

(18) He, L.; Zhang, S.; Hu, J.; Li, Z.; Zheng, X.; Cao, Y.; Xu, G.; Yan, M.; Wu, Y. On-road emission measurements of reactive nitrogen compounds from heavy-duty diesel trucks in China. *Environmental Pollution.* 2020; 114280. Available from: https://doi.org/10.1016/j.envpol.2020.114280.

(19) Misra, C.; Collins, J. F.; Herner, J. D.; Sax, T.; Krishnamurthy, M.; Sobieralski, W.; Burntizki, M.; Chernich, D. In-use NO_x emissions from model year 2010 and 2011 heavy-duty diesel engines equipped with aftertreatment devices. *Environmental Science & Technology.* 2013; 47 (14): 7892-7898. Available from: https://doi.org/10.1021/es4006288.

(20) Tan, Y.; Henderick, P.; Yoon, S.; Herner, J.; Montes, T.; Boriboonsomsin, K.; Johnson, K.; Scora, G.; Sandez, D.; Durbin, T. D. On-Board Sensor-Based NO_x Emissions from Heavy-Duty Diesel Vehicles. *Environmental Science & Technology.* 2019; 53 (9): 5504-5511. Available from: https://doi.org/10.1021/acs.est.8b07048.

(21) Zhang, S.; Zhao, P.; He, L.; Yang, Y.; Liu, B.; He, W.; Cheng, Y.; Liu, Y.; Liu, S.; Hu, Q.; Huang, C.; Wu, Y. On-board monitoring (OBM) for heavy-duty vehicle emissions in China: Regulations, early-stage evaluation and policy recommendations. *Science of The Total Environment.* 2020; 139045. Available from: https://doi.org/10.1016/j.scitotenv.2020.139045.

(22) Chan, C. C. The state of the art of electric and hybrid vehicles. *Proceedings of the IEEE.* 2002; 90 (2): 247-275. Available from: https://doi.org/10.1109/5.989873.

(23) Hallmark, S. L.; Wang, B.; Sperry, R. Comparison of on-road emissions for hybrid and regular transit buses. *Journal of the Air & Waste Management Association.* 2013; 63 (10): 1212-1220. Available from: https://doi.org/10.1080/10962247.2013.813874.

(24) Zhang, S.; Wu, Y.; Liu, H.; Huang, R.; Yang, L.; Li, Z.; Fu, L.; Hao, J. Real-world fuel consumption and CO2 emissions of urban public buses in Beijing. *Applied Energy.* 2014; 113 1645-1655. Available from: https://doi.org/10.1016/j.apenergy.2013.09.017.

(25) Suarez-Bertoa, R.; Astorga, C. Impact of cold temperature on Euro 6 passenger car emissions. *Environmental Pollution.* 2018; 234 318-329. Available from: https://doi.org/10.1016/j.envpol.2017.10.096.

(26) Grange, S. K.; Farren, N. J.; Vaughan, A. R.; Rose, R. A.; Carslaw, D. C. Strong Temperature Dependence for Light-Duty Diesel Vehicle NOx Emissions. *Environmental Science & Technology.* 2019; 53 (11): 6587-6596. Available from: https://doi.org/10.1021/acs.est.9b01024.

(27) National Atmospheric Emissions Inventory. Emissions Factors For All Alternative Vehicle Technologies. 2013. Available from: https://naei.beis.gov.uk/data/ef-transport [Accessed 15 July 2020].

(28) Notter, B.; Keller, M.; Althaus, H.; Cox, B.; Knörr, W.; Heidt, C.; Biemann, K.; Räder, D.; Jamet, M. The Handbook of Emission Factors for Road Transport (HBEFA) 4.1. Available from: https://www.hbefa.net/e/index.html.

(29) United States Environmental Protection Agency. Motor Vehicle Emission Simulator (MOVES). Available from: https://www.epa.gov/moves.

(30) Cheng, Y.; He, L.; He, W.; Zhao, P.; Wang, P.; Zhao, J.; Zhang, K.; Zhang, S. Evaluating on-board sensing-based nitrogen oxides (NO_x) emissions from a heavy-duty diesel truck in China. *Atmospheric Environment*. 2019; 216 116908. Available from: https://doi.org/10.1016/j.atmosenv.2019.116908.

(31) Met Office. Weather Observation Website. Available from: https://wow.metoffice.gov.uk/.

(32) United States Environmental Protection Agency. Regulations Requiring Onboard Diagnostic Systems on 2010 and Later Heavy-Duty Engines Used in Highway Vehicles Over 14,000 Pounds; Revisions to Onboard Diagnostic Requirements for Diesel Highway Vehicles Under 14,000 Pounds. 2008; Available from: https://nepis.epa.gov/Exe/ZyPDF.cgi/P1002LTD.PDF?Dockey=P1002LTD.PDF.

(33) Ghaffarpasand, O.; Beddows, D. C. S.; Ropkins, K.; Pope, F. D. Real-world assessment of vehicle air pollutant emissions subset by vehicle type, fuel and EURO class: New findings from the recent UK EDAR field campaigns, and implications for emissions restricted zones. *Science of The Total Environment.* 2020; 139416. Available from: https://doi.org/10.1016/j.scitotenv.2020.139416.

(34) Bayindir, K. Ç.; Gözüküçük, M. A.; Teke, A. A comprehensive overview of hybrid electric vehicle: Powertrain configurations, powertrain control techniques and electronic control units. *Energy Conversion and Management.* 2011; 52 (2): 1305-1313. Available from: https://doi.org/10.1016/j.enconman.2010.09.028.

(35) Ko, J.; Jin, D.; Jang, W.; Myung, C.; Kwon, S.; Park, S. Comparative investigation of NOx emission characteristics from a Euro 6-compliant diesel passenger car over the NEDC and WLTC at various ambient temperatures. *Applied Energy.* 2017; 187 652-662. Available from: https://doi.org/10.1016/j.apenergy.2016.11.105.

(36) Jaguemont, J.; Boulon, L.; Dubé, Y. A comprehensive review of lithium-ion batteries used in hybrid and electric vehicles at cold temperatures. *Applied Energy.* 2016; 164 99-114. Available from: https://doi.org/10.1016/j.apenergy.2015.11.034.

(37) Kotz, A. J.; Kittelson, D. B.; Northrop, W. F. Lagrangian Hotspots of In-Use NOx Emissions from Transit Buses. *Environmental Science & Technology*. 2016; 50 (11): 5750-5756. Available from: https://doi.org/10.1021/acs.est.6b00550.

(38) Keramydas, C.; Papadopoulos, G.; Ntziachristos, L.; Lo, T.; Ng, K.; Wong, H. A,; Wong, C. K. Real-world measurement of hybrid buses' fuel consumption and pollutant emissions in a metropolitan urban road network. *Energies.* 2018; 11 (10): 2569. Available from: https://doi.org/10.3390/en11102569.

(39) Department for Transport. Transport use during the coronavirus (COVID-19) pandemic. 2021; Available from: https://www.gov.uk/government/statistics/transport-use-during-the-coronavirus-covid-19-pandemic [Accessed 28 June 2021].